# Synthesis of Ag -ZnO nanocomposite using aqueous leaf extract *Salvia officinalis*: Structural characterization, cytotoxicity and antibacterial activity

K.Shreema<sup>a</sup>\*, R.Mathammal<sup>a</sup>

<sup>a</sup>Department of Physics, Sri Sarada College for Women (Autonomous), Salem-636 016, Tamil Nadu, India. Corresponding E-mail address: shreekrish14596@gmail.com

#### **ABSTRACT**

The green method for preparing metal and metal oxide nanoparticles is increasingly becoming popular as a result of its eco-friendliness compared with physical and chemical methods. The biomolecules inherent in plant extracts are known to serve as reductants and capping agents to form metal/metal oxide nanoparticles. In the current study, ZnO and Ag-ZnO NCs are produced by a using an aqueous leaf extract of *Salvia officinalis* plant as a reducing agent. Synthesis of nanoparticles and nanocomposites is characterized and confirmed by X-ray diffraction (XRD), ultraviolet-visible spectroscopy (UV–Vis), Fourier-transform infrared spectroscopy (FTIR), Scanning electron microscopy (SEM), energy dispersive spectroscopy (EDS) and transmission electron microscope (TEM). Then, antibacterial activity is tested against gram positive (*S. aureus and B. subtilis*) and gram negative BS (*P. aeruginosa, E. coli*) using the agar well diffusion method. Maximum inhibition zones are observed for *B. subtilis* (33 mm). These results are promising in terms of their potential ability to be used against pathogenic bacteria. The Ag-ZnO NCs showed potential cytotoxicity against HT-29 cell lines.

**Keywords:** Nanotechnology, *Salvia officinalis*, silver-zinc oxide nanocomposites, Antibacterial activity, anticancer activity.

## 1. Introduction

The advent of antibiotic-resistant bacteria and deteriorating human immunological compatibility has caused a substantial surge in the threats posed by microbial infections in recent years. Because of their low profit margins, several pharmaceutical companies have stopped investing in the development of novel antibiotic molecules. Despite the market's abundance of innovative antibiotics and therapeutics, 70% of them are ineffective at treating intracellular infections due to their decreased permeability [1], [2]. Parallel to this, the worldwide public health will be greatly impacted by the development of new or improved antibiotics and nonantibiotic materials. It is essential to develop improved biocompatibility and efficiency therapeutic agents to overcome these problems [3]. Nanoparticles are increasingly regarded as effective antibacterial agents and appear to have enormous promise to address the issues associated with microbial multidrug resistance [4], [5]. The nanotechnology is one of the most important emerging field in modern materials science, especially in biotechnology [6], [7]. Using green synthesis methods, nanoparticles can be synthesized without harsh chemicals or toxic by-products and then functionalized without hazardous chemicals. Hence, green synthesized NPs can be suitable for biomedical applications [8]. In terms of large-scale nanoparticle biosynthesis, plant biomaterials seem to be the most suitable among various natural resources. Furthermore, plant-mediated synthesis involves no specific conditions and does not require any special equipment. Additionally, plant produce more diverse nanoparticles compared to other bio-organisms in terms of size and shape [9]. In plant extracts, bioactive constituents

like flavonoids, glycosides, alkaloids, phenolic, acids, terpenoids amino acids, proteins and enzymes play a key role in the formation and stabilization of various compounds [10]. A major advantage of nanotechnology is its ability to modify and develop the properties of metals by converting them into their nanoforms (nanoparticles), which could be used to treat different diseases.

Biosynthesized nanoparticles possess a wide range of physicochemical characteristics, such as their size distribution, shape, chemical composition, surface charge and surface chemistry, which are important for pharmaceutical properties, cellular interactions and toxic manifestations. In addition, various plant sources that act as bio-reducing and bio capping agents in the green synthesis may affect the biological activity [11], [12]. Variations in these factors can result in different cytotoxic effects [13]. *Salvia officinalis* is an evergreen perennial shrub with some medicinal and culinary [14]. The medicinal uses include; pain reliever, antioxidant, anti-inflammatory, antimicrobial and antiviral agents [15], [16]. Some studies carried out by researchers from other countries have reported on *S. officinalis*-mediated silver nanoparticles synthesis [17]. To the best of our knowledge, this is the first study reporting on synthesis of Ag-ZnO NCs from *S. officinalis* leaf extract. Therefore, in this present study, an aqueous extract of *S. officinalis* is used to synthesize ZnO NPs and Ag-ZnO NCs and subsequently, several techniques are used for its characterization and its cytotoxic effect on HT-29 cells line and antibacterial activity determination.

#### 2. Materials and Methods

## 2.1 Preparation of Leaf extract

Salvia officinalis leaves are gathered from surrounding areas of Dharmapuri, Tamil Nadu. 20g of leaves are taken and washed with distilled water. Then it is allowed to boil at 60°C for 30 min. Whatman filter paper is used to filter the leaf extract and stored for future studies [18].

# 2.2 Preparation of zinc oxide nanoparticles

0.35 M of zinc acetate dihydrate along with 10 ml of leaf extract was dissolved in 100 ml of double distilled water and allowed to stir for 30 min using magnetic stirrer. The pH of the solution was kept constant at 13 by adding few drops of sodium hydroxide solution. The pale white color was obtained and after complete stirring, the solution gets precipitated. The particle was washed thrice using distilled water inorder to remove impurities. After the particle gets dried using hot air oven at 80°C for 3 Hrs and at muffle furnace for 4 Hrs at 400°C. Finally, the particle was grinded in a mortar to produce fine nanoparticles [20].

# 2.3 Preparation of silver - zinc oxide nanocomposite

Silver nitrate at different concentrations (0.05 M, 0.1 M, 0.15 M, 0.2 M, 0.25 M) were taken along with 0.35 M of Zinc acetate dihydrate and 10 ml of leaf extract was dissolved in 100 ml of distilled water and allowed to stir for 30 min using magnetic stirrer. The pH of the solution was kept constant at 13 by adding few drops of sodium hydroxide solution. The dark brown color was obtained and after complete stirring, the solution gets precipitated. The similar drying procedure was carried out for Ag-ZnO nanoparticles.

## 3. Characterization Techniques

Various analysis techniques are used to confirm the synthesis of ZnO NPs and Ag-ZnO NCs. It is evaluated with the  $\underline{XRD}$  pattern (Inel Equinox 2000 diffractometer) which is used to check the crystal structure and determine the phases. The visual properties of NPs are determined

by UV–Vis (Perkin Elmer Lambda 35). FT-IR spectrum (Perkin Elmer spectrum two) to identify bonds and functional groups that existed in the range of 400–4000 cm<sup>-1</sup>.FESEM/EDAX is used to determine the morphology and size of NPs (EV018, Carl Zeisis). Then, zone of inhibition is determined by agar well diffusion method (discussed in chapter 3.3.1). The toxicity of ZnO NPs and Ag-ZnO NCs are assessed on HT-29 cells by the MTT procedure (discussed in chapter 3.3.2).

## 4. Result and Discussion

# 4.1 X-ray diffraction analysis

Figure 1 shows the XRD patterns of ZnO and Ag–ZnO nanocomposites with various Ag concentrations (0.05, 0.1, 0.15, 0.2 and 0.25 M). The ZnO patterns display diffraction peak positions at  $2\theta$  values of 31.48°, 34.29°, 36.02°, 47.29°, 56.6°, 62.68° and 67.8° which are indexed to the crystal planes (100), (002), (101), (102), (110), (103) and (112) of hexagonal wurtzite structures and has good agreement with JCPDS file no. 36-1451 [19]. Furthermore, the Ag-ZnO nanocomposite exhibits four additional peaks upon doping with different concentrations of Ag salts, at 37.5°, 44.04°, 64.2°, and 77.2° correspond to (111), (200), (220), and (311) planes, respectively [20] and well matched with JCPDS, card No. 04-0783 [21], [22], confirming the existence of metallic Ag in Ag-ZnO nanocomposites. The peak intensity gradually increases with an increase in the Ag content, which signifies the successful formation of Ag nanoparticles on the ZnO surface [23] and shows in Figure 2. The peak intensity of Ag phase for Ag-ZnO nanocomposites is intensified and sharper with the increment of Ag contents, which suggest that Ag metallic phase has been successfully formed on the surface of ZnO-NPs rather than incorporation into the ZnO lattice. This could be due to the fact that the ionic radius of Ag + (126 pm) is larger than that of Zn<sup>2+</sup>(74 pm), which resulted to the formation of metallic Ag, and no shift in the peak positions of Ag–ZnO nanocomposites indicates that Ag particles are positioned on the surfaces of well crystalline ZnO-NPs [24]. The patterns seen in Figure 1 suggest that the structure of ZnO and Ag-ZnO NCs is face-centered cubic (fcc) and the space group is P63mc and the other phases did not have any additional peaks, which indicates that there is no impurity in the product, which is connected to the EDX results [25].

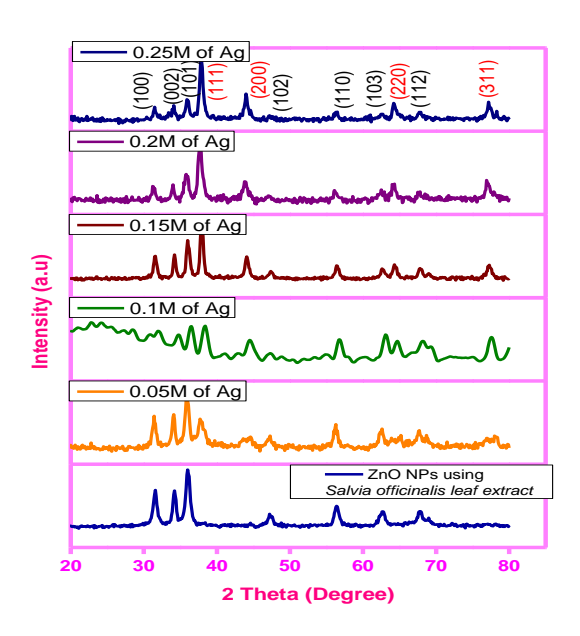


Figure 1: XRD pattern of ZnO and Ag -ZnO NCs using Salvia officinalis

The particle size is increased with increasing Ag content which is estimated by the Scherer formula.

$$D = \frac{k\lambda}{\beta_{\rm d} \cos \theta} \text{ nm}$$

The average particle size of ZnO NPs using *Salvia officinalis* leaf extract is 12.14 nm. The results are well matched with Abomuti et al [26] and Alrajhi et al [27] who reported the average crystallite size of ZnO NPs is calculated to be 11.89 nm and 12.06 nm, respectively using *Salvia officinalis* leaf extract. The increase in crystal size from 0.05 M to 0.25 M of Ag–ZnO NCs might be attributed to the Ag anchoring on the ZnO surface. As Ag content increases, the crystalline size increases from 11.14 to 15.52 nm and summarized in **Table 1.** Hence the crystallite size of the ZnO nanoparticles enhanced with Ag doping.

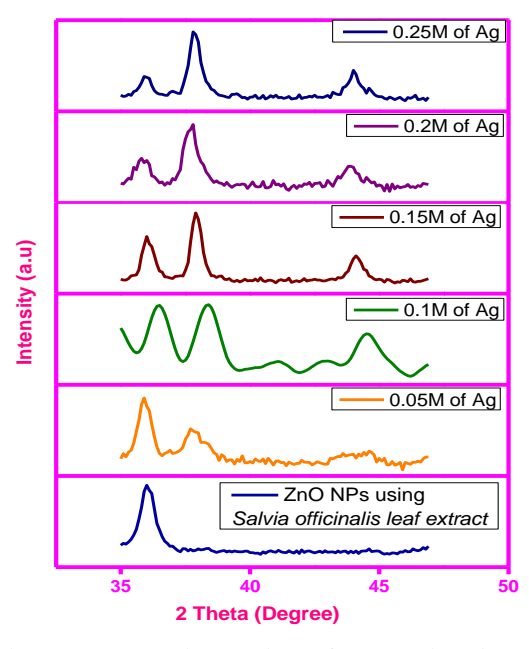


Figure 2: The intensity of peaks is slightly increased with increasing the concentration of silver.

Table 1: XRD parameters of ZnO and Ag-ZnO NCs

Samples	'd'	Lattice		c/a ratio	Unit cell	Particle	System/Space
name	spacing (Å)	Parame	eters		volume (Å) <sup>3</sup>	size (nm)	group
Undoped ZnO	2.65	3.66	5.29	1.44	62.627	12.14	Hexagonal /P6 <sub>3</sub> mc
0.05 M of Ag	2.66	3.69	5.31	1.44	63.33	11.14	
0.1 M of Ag	2.56	3.56	5.13	1.44	57.38	11.78	
0.15 M of Ag	2.37	3.29	4.74	1.44	44.55	12.29	
0.2 M of Ag	2.32	3.22	4.63	1.44	42.38	15.16	
0.25 M of Ag	2.31	3.21	4.62	1.44	41.94	15.52	

# 4.2 UV-Visible spectroscopy

The size, shape, interaction between the particles, and the absorbed molecules present on the surface of the nanoparticles has a strong influence on the optical properties of metal nanoparticles. The growth of green synthesized ZnO and Ag-ZnO NCs is monitored by observing changes in the color of reaction mixture. For ZnO NPs the color changes from light green to pale yellow color and for Ag-ZnO NCs, the color changes from light green to dark brown color. The change of color indicates the formation of NPs and due to the surface plasmon resonance in which the vibration of free electrons on its surface. The absorption wavelength and band gap energy of ZnO and Ag- ZnO NCs are determined by using UV-Vis spectroscopy [28]. Figure 3 shows that absorption spectrum of ZnO and Ag-ZnO NCs. The absorption wavelength for ZnO Nps is 367.08 nm. Figure 4 and Figure 5 shows the absorption wavelength Vs band gap energy for various concentrations of Ag- ZnO NCs. The result is well matched with Abomuti et al [26] who reported that S. officinalis extract-mediated ZnO NPs shows an absorption peak at 368 nm. Table 2 represents the absorption wavelength and band gap energy of ZnO and Ag-ZnO NCs. The band gap energy is found to be 3.38 eV for ZnO NPs and for Ag doped materials, the energy is gradually decrease from 3.46 to 3.07 eV. Therefore from the results, the red shift is observed for Ag- ZnO NCs indicating the reduction of band gap energy.

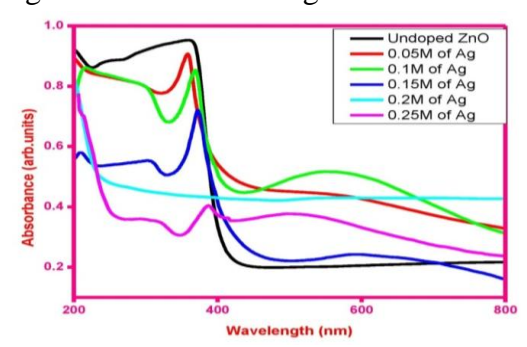


Figure 3: UV-Visible analysis of ZnO and Ag -ZnO NCs using Salvia officinalis

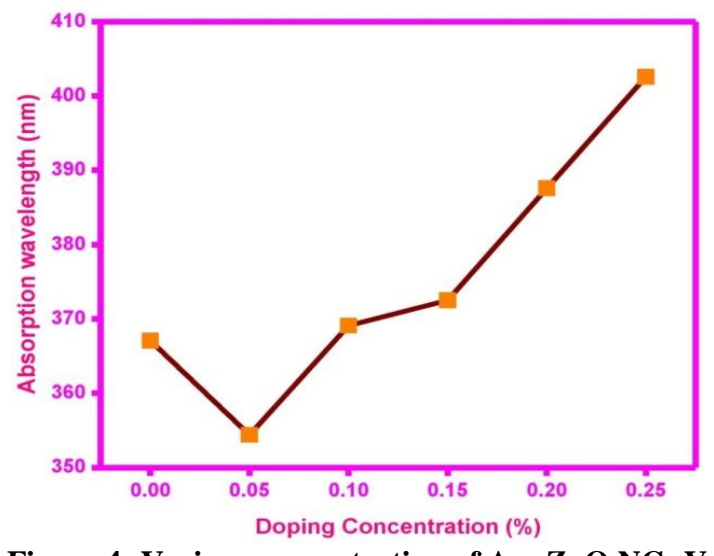


Figure 4: Various concentration of Ag -ZnO NCs Vs band gap energy

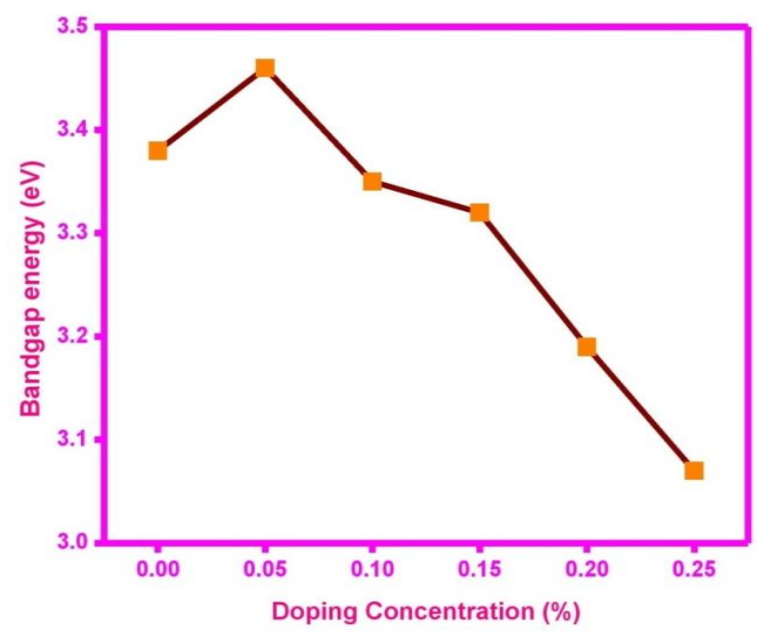


Figure 5: Various concentration of Ag -ZnO NCs Vs absorbance wavelength

As the concentration of deposited Ag gradually increased, the absorption intensity also gradually increased from 350 to 410 nm [29]. Due to presence of oxygen vacancies, band gap energy is decreased for Ag- ZnO NCs. The same result is obtained with Bechambi et al. [30] in which the band gap energy is decreased from 3.28 eV to 3.21 eV with the increase of Ag doping level. The Bechambi et al. explain this by changing the crystalline structure of ZnO, which was slightly influenced by the inclusion of ionic Ag [31]. According to the results from our experiment the decrease in the band gap can be explained by distortion of the crystalline structure of ZnO, results that are in good agreement with the XRD analysis.

Table 2: Absorption wavelength and Bandgap energy of ZnO and Ag-ZnO NCs

S.No.	Sample name	Absorption wavelength (nm)	Bandgap energy (eV)
1	Undoped ZnO	367.08	3.38
2	0.05 M of Ag-ZnO	354.4	3.46
3	0.1 M of Ag-ZnO	369.1	3.35
4	0.15 M of Ag-ZnO	372.5	3.32
5	0.2 M of Ag-ZnO	387.6	3.19
6	0.25 M of Ag-ZnO	402.6	3.07

## 4.3 Fourier Transform Infra-Red Spectroscopy

The presence of active biomolecules in *Salvia officinalis* leaf extract act as reducing and capping agent during the biosynthesis of nanomaterials. Characterization and an explanation of the functional groups involved in the synthesis, reduction and stabilization of ZnO and Ag-ZnO NCs are accomplished with the assistance of FT-IR spectroscopy [32]. **Figure 6** shows the FTIR spectrum of ZnO and Ag-ZnO NCs. Specifically, a prominent peak is detected at 3446.79 cm<sup>-1</sup> analogous to the stretching vibration of –OH and NH<sub>2</sub> group. These functional groups are

produced from water and leaf extract of *Salvia officinalis* [33]. The absorption peaks at 2916.796, and 1637.56 cm<sup>-1</sup> correspond to the C–H stretching and C=O stretching mode of the carbonyl group respectively, [34], [35], [36].

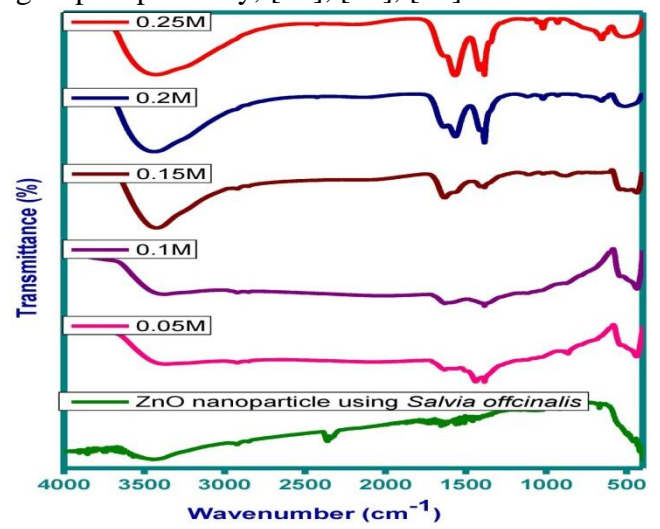


Figure 6: FTIR spectra of ZnO and Ag -ZnO NCs using Salvia officinalis leaf extract

The adsorption peaks at 1557.54 cm<sup>-1</sup> are due to the C=C stretching of alkene present in the aromatic ring structure. The band at 678.94 cm<sup>-1</sup> represents the aromatic C–H out of plane bending in polyphenols. Alkaloid compounds work as weak base due to presence of nitrogen atoms in cyclic rings which provide electrons pairs to react with water molecules to produce OH ions which hydrolyses or reduces the metal ions. On the other hand, the OH bending and OH stretching depict the presence of flavonoids, tannins, and saponins, in *Salvia officinalis* extract which act as capping agents to prevent agglomeration and thus control the particle size. During nanoparticles formation the OH hydrophilic head of phytocompounds interact with metal ions whereas hydrophobic part provides a steric hindrance that prevent the agglomeration of nanoparticles [37]. Apart from the OH groups, studies have shown that the C=C and C=O groups from the phytocompounds can work as a capping agents [23]. Furthermore, it has been observed that the formation of ZnO nanoparticles and Ag–ZnO nanocomposites provides an insight of the participation of biomolecules in the reduction and stabilization of the nanomaterials. Collectively, FTIR analysis affirmed that the phenols, alcohols, amines, and alkanes of the plant extract act as reducing, stabilizing, and capping agents for ZnO and Ag-ZnO NCs.

## 4.4 Scanning electron microscopy

Surface morphology is one of the important properties of thin films and nanomaterials which plays a decisive role in the selection of materials for fabricating various devices [38]. **Figure 6.7** show the morphology of ZnO NPs which is spherical in shape and for Ag–ZnO NCs, the particles exhibit spherical with slightly agglomerate. This accumulation is common among NPs synthesized by green chemistry procedure and is due to their higher surface area and stable association that lead to the inducement of aggregation or agglomeration [39]. The SEM micrograph distinctly specifies the occurrence of agglomeration and established a similitude in the morphology of ZnO and Ag-ZnO NCs. This similitude is a result of the uniform distributions of Ag on the surface of ZnO NPs. The formation of a greyish-white patch on top of the samples indicates the diffusion of metal ions on the surface of the ZnO NPs [40]. The images are captured at different magnifications. The synthesized NPs well dispersed, and the effective dispersion of particles is one of the factors that are influenced in the test environment and are used in applications such as cytotoxicity and heterogeneous catalysts [41].

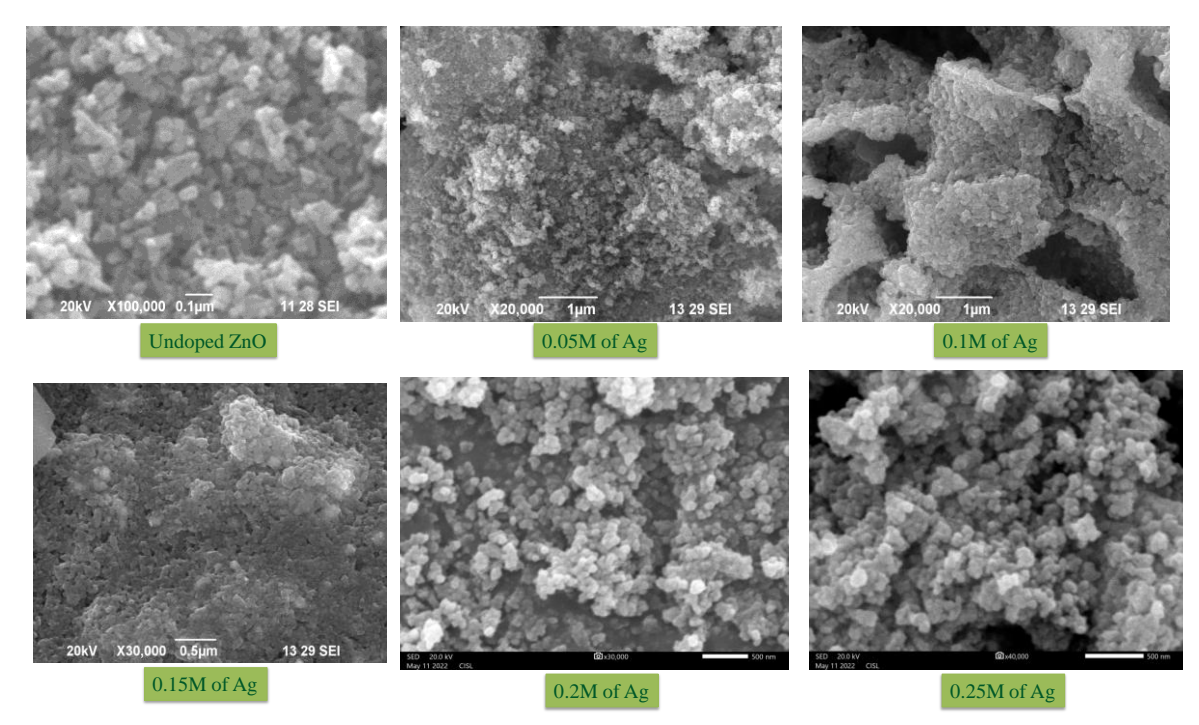


Figure 7: Surface Morphology of ZnO and Ag -ZnO NCs using Salvia officinalis leaf extract

## 4.5 Energy Dispersive X-ray Analysis

When the electromagnetic radiations of higher energy (X-Rays) fall on the sample the "core" electrons from the atom eject out leaving behind holes. These holes are occupied with higher energy electrons which release energy during this process. This energy is different for each element which can be captured to identify the presence along with the proportion of elements [42].

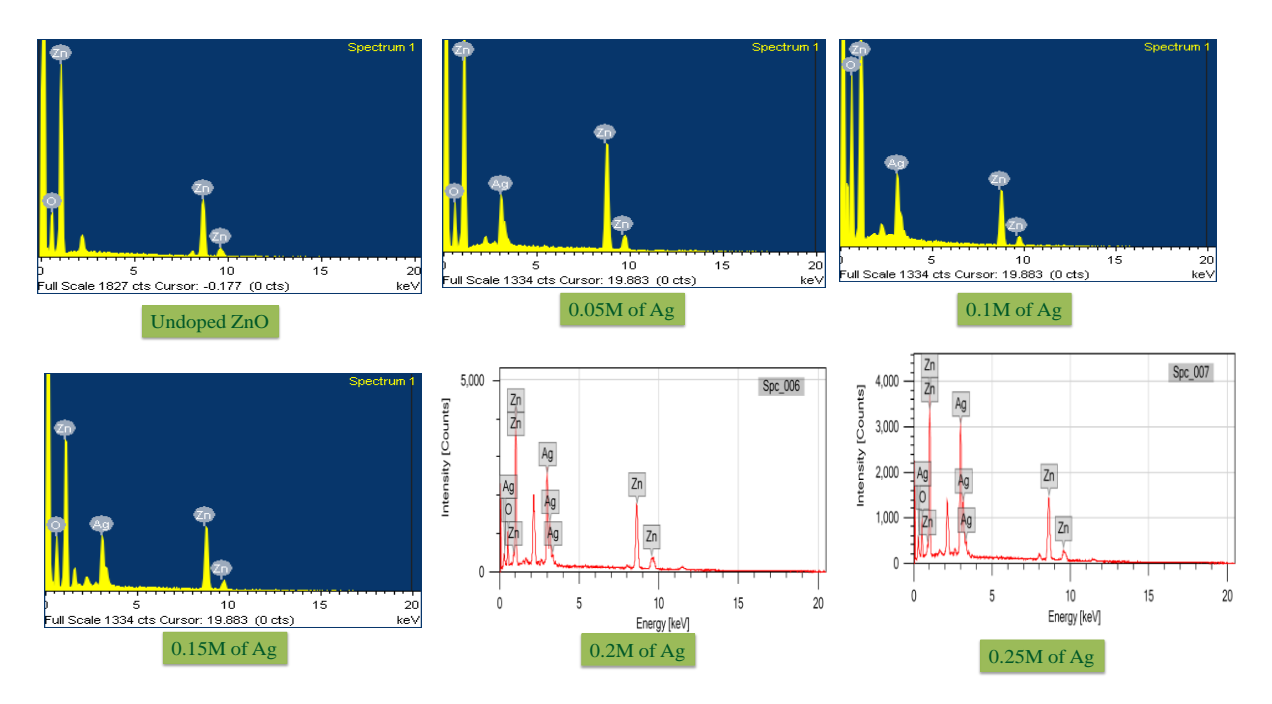


Figure 8: EDX micrographs of ZnO and Ag -ZnO NCs using Salvia officinali leaf extract

The elemental composition of ZnO and Ag- ZnO NCs are determined via the utilization of EDX analysis. The peaks corresponding to Zn and O are observed at signals 0 and 2 keV, respectively and two peaks of Zn are found in between 8 and 10 keV which is shown in **Figure 8**. Conversely, the signals detected at 3 keV are attributed to Ag NPs. From the above result which suggests that the biosynthesis method utilizing *Salvia officinalis* leaf extract is highly effective. The non-existence of other elements indicates that the pure phase of NPs is created.

#### 4.6 Antibacterial activity

The biogenic zinc oxide nanoparticles have also shown significant antibacterial potential against various bacterial strains (BS). The activity is done against different gram positive (*S. aureus and B. subtilis*) and gram negative BS (*P. aeruginosa, E. coli*). No single dose has shown stronger potential than positive control. The increased antibacterial potential of ZnO NPs is due to the bioactive functional groups attached on the surface of NPs.

Table 3: Antibacterial activity of ZnO and Ag-ZnO NCs using fresh leaf extract Salvia officinalis

S.No	Organisms	Sample name					
		Undoped ZnO	0.05M of Ag	0.1M of Ag	0.15M of Ag	0.2M of Ag	0.25M of Ag
1.	Bacillus subtilis	23	24	26	27	29	33
2.	S. aureus	14	18	20	21	24	25

3.	E.coli	12	16	18	19	22	24
4.	Pseudomonas aeruginosa	17	18	20	22	23	26

Besides, different functional groups attached in Salvia officinalis leaf extract which act as a capping agent of ZnO NPs, which play an important role in the bacterial inhibition. The zone of inhibition values of Ag-ZnO nanocomposites is undeniably higher than pure ZnO NPs for all strains. This demonstrates the higher antibacterial activity of Ag–ZnO nanocomposites over ZnO nanoparticles, which is attributed to their synergic effect. Furthermore, the antibacterial activity of Ag-ZnO nanocomposites is found to increase with the increase in Ag concentrations. This confirms that doping of Ag in ZnO improves the antibacterial activity of ZnO nanoparticles. Here with, the phenomenon can be ascribed to the stronger antimicrobial effect of Ag. The maximum zone of inhibition values recorded by Ag-ZnO is B. subtilis (33 mm) and minimum zone of inhibition values recorded by E.coli (24 mm) and summarized in Table 3. From the above result, the synergic antibacterial activity found to be more prominent against Grampositive bacteria than gram negative bacteria. The antibacterial activities of ZnO NPs differ depending on the cell wall nature of Gram-positive bacteria or gram .negative bacteria. A similar trend is obtained by Vijayakumar et al. [43] who stated that ZnO NPs synthesized from Laurus nobilis leaf extract displayed greater antibacterial activity against gram positive bacteria (S. aureus) than gram negative bacteria (P. aeruginosa). They suggested that the outer thick peptidoglycan layer and other surface components of gram-positive bacteria may promote ZnO attachment onto the cell wall whereas the components of gram-negative bacteria may repeal this attachment [44]. The possible Inhibitory action is physical damage caused by interaction of the material with outer cell wall layer increased by increased concentration of Ag-ZnO NPs [45].

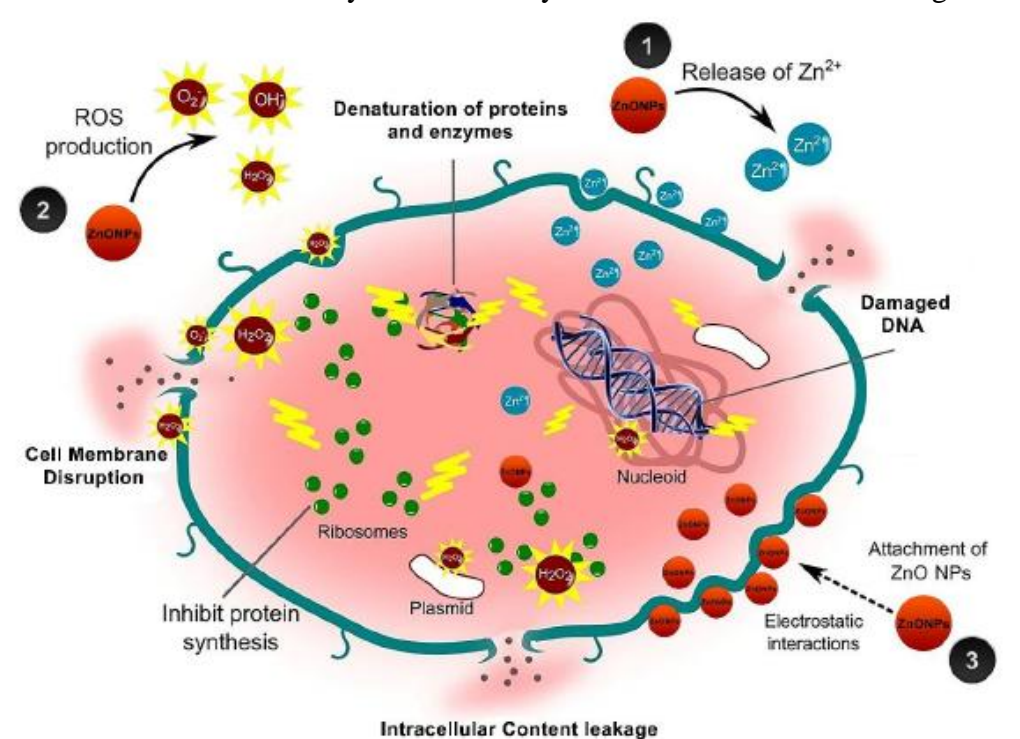


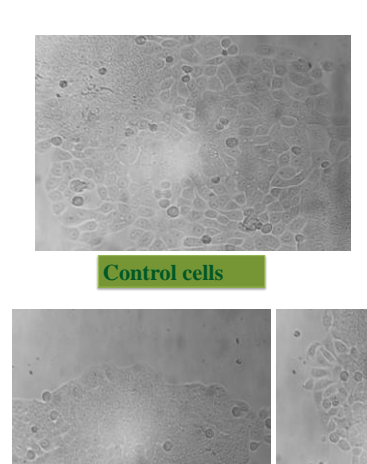
Figure 9: Various proposed mechanisms of ZnO NPs toxicity against bacteria

For the effect of ZnO NPs, there are some proposed bactericidal mechanisms (**Figure 9**) that have been suggested by scientists. Some suggested that the released Zn from ZnO NPs possess toxic properties that are leading to inhibiting a lot of bacterial cell activities such as bacterial metabolism, and enzyme activity resulting in cell bacterial death [46], [47]. The other suggested mechanism is the formation of reactive oxygen species (ROS) that activates oxidative stress which subsequently leads to cell death [48], [49]. Another proposed mechanism is the lethal activity of the ZnO NPs due to the attachment of the NPs to the bacterial cell membranes, and the accumulation inside the cytoplasm resulting in damaging the cell membrane integrity and loss of cell contents because of the leakage ending up with cell death [50]. Finally, it can be concluded that that the contact of prepared NPs with the cell wall surfaces of bacteria causes the Ag+ and Zn2+ and forms ROS; it results in the rupture of the cell wall [51].

# 4.7 Anticancer activity

Cancer is a fatal disease, a major cause of deaths around the globe, and is continuously increasing in cause of death by an estimated ~21 million by the year 2030. Among the numerous types of cancers, colon cancer is presently the third deadliest cancer causes (~745,517) deaths. The different risk factors related are viral infection, extensive alcohol use, and toxin exposures (aflatoxin) [51]. The cytotoxicity potential of the synthesized zinc oxide nanoparticles against human colon cells (HT-29) is evaluated using MTT cytotoxicity assay. The key results obtained by MTT cytotoxicity assay in HT-29 cells treated with various doses of ZnO and Ag- ZnO NCs ranging from 5-500 µg/mL for 24 hrs are summarized in **Tables 4 and 5**. Our results of ZnO and Ag- ZnO NCs have determined strong reduction in the metabolic activity of HT-29 cancer cells. The metabolic activity is reducing continuously with increase in ZnO and Ag- ZnO NCs concentrations. The highest cell viability (~12.36 %) is achieved at 500µg/mL for Ag- ZnO NCs. The reduction in metabolic activity has shown that ZnO and Ag- ZnO NCs might have potential anticancer activity [52]. The IC<sub>50</sub> value recorded for Salvia officinalis mediated ZnO and Ag-ZnO NCs against HT-29 cell lines is 73.59 and 58.74 µg/mL, respectively. The results obtained from this study are also very well supported with various evidences for the cytotoxic effect of green ZnO NPs using Salvia officinalis leaf extract against the colon cancer (HT-29 cell line) [52,53]. Yesilot et al [53] reported that MTT results showed that Salvia officinalis leaf extract have higher cytotoxic activity in MCF-7 breast cancer cell lines than in CRL-4010 human breast epithelial cells (IC50 values 8.49 and 9.69 µg/mL, respectively). Fatemeh Sharifi et al [54] reported that Synthesis of silver nanoparticles using Salvia officinalis extract has cytotoxic on cell lines with approximate IC<sub>50</sub> values of 240, 58.60 and 50.40 µg/mL in Hek-293, A-172 and MCF 7 cell lines, respectively. These values indicate that AgNPs have a potent cytotoxic activity towards studied human cell lines. The findings of the MTT assay show that the cytotoxic effect depends on the dose of NPs and can dramatically destroy cancer cells. The images of cell viability of ZnO and Ag-ZnO NCs using Salvia officinalis against HT-29 cell lines for various concentrations are shown in Figures 10 and 11, respectively.

S. No	Tested sample concentration (µg/ml)	Cell viabilit (in triplicat	Mean Val	lue		
1.	Control	100	100	100	100	



100 μg/ml

Figure 10: Anticancer activity of ZnO nanoparticles

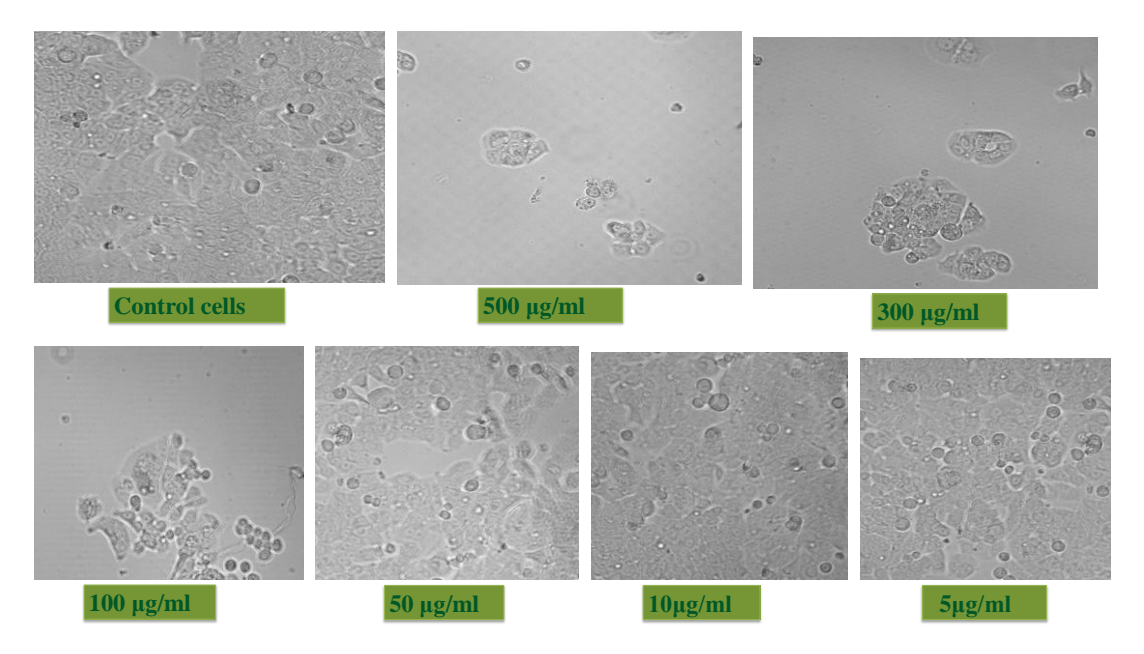


Figure 11: Anticancer activity of Ag-ZnO NCs (0.25M) using fresh leaf extract *Salvia officinalis* 

Table 4: Anticancer activity of ZnO NCs

2.	500 μg/ml	14.6051	14.4131	13.7048	14.240987
3.	400 μg/ml	24.4411	23.9227	23.7952	24.053016
4.	300 μg/ml	34.4262	34.6211	34.488	34.51176
5.	200 μg/ml	43.07	43.685	43.2229	43.325976
6.	100 μg/ml	47.2429	46.211	47.2892	46.914358
7.	50 μg/ml	56.7809	56.9094	57.0783	56.922866
8.	25 μg/ml	62.4441	62.11	61.4458	61.999951
9.	15 μg/ml	69.5976	70.1337	71.3855	70.372296
10.	10 μg/ml	82.8614	77.8603	79.3675	80.029733
11.	5 μg/ml	94.4858	93.3135	93.0723	93.623884

Table 5: Anticancer activity of Ag-ZnO NCs (0.25M) using fresh leaf extract Salvia officinalis

S. No	Tested sample concentration (µg/ml)	Cell viability ( (in triplicates)	Mean Value (%)		
1.	Control	100	100	100	100
2.	500 μg/ml	12.3924	11.0124	13.6824	12.362431
3.	400 μg/ml	19.9656	19.0053	20.9459	19.972284
4.	300 μg/ml	26.3339	29.6625	29.8986	28.631693
5.	200 μg/ml	40.6196	39.254	34.6284	38.167332
6.	100 μg/ml	51.1188	50.7993	48.8176	50.245206
7.	50 μg/ml	57.6592	57.3712	53.8851	56.30519
8.	25 μg/ml	66.4372	66.4298	63.5135	65.460177
9.	15 μg/ml	70.9122	76.7318	71.6216	73.088545
10.	10 μg/ml	81.9277	82.0604	82.9392	82.309097
11.	5 μg/ml	88.1239	90.0533	88.3446	88.840602

#### **Conclusion**

The green approach has been adopted to synthesize ZnO NPs and Ag-ZnO NCs using the aqueous leaf extract from *Salvia officinalis*. The formation of Ag-ZnO NCs is confirmed by XRD, UV-Vis spectrophotometry, FTIR, SEM and EDX. Different antimicrobial activities of Ag-ZnO nanocomposites are investigated and found to have higher antimicrobial activity against *B. subtilis* than *E.coli* bacteria. The Ag-ZnO nanocomposites presented higher antimicrobial properties compared to ZnO nanoparticles. This provides an insight that the addition of silver (Ag) nanoparticles improves the antimicrobial activity of the Ag-ZnO nanocomposites especially for *B. subtilis* (gram-positive bacteria). The anticancer activity of ZnO NPs and Ag-ZnO NCs that have been synthesized from the *Salvia officinalis* leaf extract is demonstrated in a human colon cancer cell line with an IC 50 value of 73.59 and 58.74 µg/mL, respectively. Based on the above findings, we can say that green synthesis is the way forward and new frontier for designing nanomedicine and can be utilized in different theranostic applications for the treatment

of different diseases. In addition, in vivo studies are encouraged on toxicity aspects in different animal models, and once their biocompatibility and bio-safe nature is confirmed, only then can these NPs can be utilized in clinical applications. Further studies are encouraged on the mechanistic and synthesis aspects of the ZnO NPs and Ag-ZnO NCs by using different medicinal plant materials.

#### References

- [1] J. Samuel, M. M. Selvam, K. Manigundan, B. Abirami, S. Thangavel, and R. K. Manikkam, "Biosynthesis, Characterization and Evaluation of Antimicrobial, Antioxidant and Antiproliferiative Activities of Biogenic Silver Nanoparticles Using Streptomyces KBR3," *Indian J. Pharm. Sci.*, vol. 85, no. 1, pp. 23–30, Feb. 2023, doi: 10.36468/pharmaceutical-sciences.1064.
- [2] E. Sánchez-López *et al.*, "Metal-based nanoparticles as antimicrobial agents: an overview," *Nanomaterials*, vol. 10, no. 2, p. 292, 2020.
- [3] M. Wypij, J. Czarnecka, M. Świecimska, H. Dahm, M. Rai, and P. Golinska, "Synthesis, characterization and evaluation of antimicrobial and cytotoxic activities of biogenic silver nanoparticles synthesized from Streptomyces xinghaiensis OF1 strain," *World J. Microbiol. Biotechnol.*, vol. 34, pp. 1–13, 2018.
- [4] M. Rai, A. Yadav, and A. Gade, "Silver nanoparticles as a new generation of antimicrobials," *Biotechnol. Adv.*, vol. 27, no. 1, pp. 76–83, 2009.
- [5] G. Franci *et al.*, "Silver nanoparticles as potential antibacterial agents," *Molecules*, vol. 20, no. 5, pp. 8856–8874, 2015.
- [6] H. Erjaee, H. Rajaian, and S. Nazifi, "Synthesis and characterization of novel silver nanoparticles using Chamaemelum nobile extract for antibacterial application," *Adv. Nat. Sci. Nanosci. Nanotechnol.*, vol. 8, p. 025004, May 2017, doi: 10.1088/2043-6254/aa690b.
- [7] D. Jain, H. K. Daima, S. Kachhwaha, and S. L. Kothari, "Synthesis of plant-mediated silver nanoparticles using papaya fruit extract and evaluation of their anti microbial activities," *Dig. J. Nanomater. Biostructures*, vol. 4, no. 3, pp. 557–563, 2009.
- [8] M. Saravanan *et al.*, "Emerging antineoplastic biogenic gold nanomaterials for breast cancer therapeutics: a systematic review," *Int. J. Nanomedicine*, pp. 3577–3595, 2020.
- [9] S. Jadoun, R. Arif, N. K. Jangid, and R. K. Meena, "Green synthesis of nanoparticles using plant extracts: A review," *Environ. Chem. Lett.*, vol. 19, pp. 355–374, 2021.
- [10] V. V. Makarov *et al.*, "'Green' nanotechnologies: synthesis of metal nanoparticles using plants," *Acta Naturae Англоязычная Версия*, vol. 6, no. 1 (20), pp. 35–44, 2014.
- [11] H. Barabadi *et al.*, "Emerging theranostic silver nanomaterials to combat lung cancer: a systematic review," *J. Clust. Sci.*, vol. 31, pp. 1–10, 2020.
- [12] H. Barabadi *et al.*, "Emerging antineoplastic gold nanomaterials for cervical cancer therapeutics: a systematic review," *J. Clust. Sci.*, vol. 31, pp. 1173–1184, 2020.
- [13] H. Barabadi, H. Vahidi, K. Damavandi Kamali, M. Rashedi, and M. Saravanan, "Antineoplastic biogenic silver nanomaterials to combat cervical cancer: a novel approach in cancer therapeutics," *J. Clust. Sci.*, vol. 31, no. 4, pp. 659–672, 2020.
- [14] C. M. Nicolescu, R. L. Olteanu, and M. Bumbac, "Growth Dynamics Study of Silver Nanoparticles Obtained by Green Synthesis using *Salvia officinalis* Extract," *Anal. Lett.*, vol. 50, no. 17, pp. 2802–2821, Nov. 2017, doi: 10.1080/00032719.2017.1325895.
- [15] W. K. Khalil and F. Abdu, "Effects of Salvia officinalis extract and its nano-encapsulated form on methylmercury induced neurotoxic-stress in male rats," *World Appl Sci J*, vol. 24, no. 7, pp. 826–837, 2013.

- [16] S. Pirtarighat, M. Ghannadnia, and S. Baghshahi, "Green synthesis of silver nanoparticles using the plant extract of Salvia spinosa grown in vitro and their antibacterial activity assessment," *J. Nanostructure Chem.*, vol. 9, no. 1, pp. 1–9, Mar. 2019, doi: 10.1007/s40097-018-0291-4.
- [17] J. Baharara, T. Ramezani, M. Mousavi, and M. Asadi-Samani, "Antioxidant and anti-inflammatory activity of green synthesized silver nanoparticles using Salvia officinalis extract," *Ann. Trop. Med. Public Health*, vol. 10, no. 5, 2017, Accessed: Sep. 27, 2023. [Online].

  Available: https://search.proquest.com/openview/5dee11fc0b9a21fd08eaa5b5e9b1a9ce/1?pq-origsite=gscholar&cbl=226528
- [18] S. Vijayakumar, G. Vinoj, B. Malaikozhundan, S. Shanthi, and B. Vaseeharan, "Plectranthus amboinicus leaf extract mediated synthesis of zinc oxide nanoparticles and its control of methicillin resistant Staphylococcus aureus biofilm and blood sucking mosquito larvae," *Spectrochim. Acta. A. Mol. Biomol. Spectrosc.*, vol. 137, pp. 886–891, 2015.
- [19] "Soto-Robles: Biosynthesis, characterization and photocata... Google Scholar." Accessed: Sep. 27, 2023. [Online]. Available: https://scholar.google.com/scholar\_lookup?title=Biosynthesis%2C%20characterization%20a nd%20photocatalytic%20activity%20of%20ZnO%20nanoparticles%20using%20extracts%2 0of%20Justicia%20spicigera%20for%20the%20degradation%20of%20methylene%20blue&journal=J.%20Mol.%20Struct.&doi=10.1016%2Fj.molstruc.2020.129101&volume=1225&publication\_year=2021&author=Soto-Robles%2CC
- [20] "Göl: Green synthesis and characterization of Camellia... Google Scholar." Accessed: Sep. 27, 2023. [Online]. Available: https://scholar.google.com/scholar\_lookup?title=Green%20synthesis%20and%20characteriz ation%20of%20Camellia%20sinensis%20mediated%20silver%20nanoparticles%20for%20a ntibacterial%20ceramic%20applications&journal=Mater.%20Chem.%20Phys.&doi=10.1016%2Fj.matchemphys.2020.123037&volume=250&publication\_year=2020&author=G%C3%B6l%2CF
- [21] "Garibo: Green synthesis of silver nanoparticles using... Google Scholar." Accessed: Sep. 27, 2023. [Online]. Available: https://scholar.google.com/scholar\_lookup?title=Green%20synthesis%20of%20silver%20na noparticles%20using%20Lysiloma%20acapulcensis%20exhibit%20high-antimicrobial%20activity&journal=Sci.%20Rep.&doi=10.1038%2Fs41598-020-69606-7&volume=10&issue=1&pages=1-11&publication\_year=2020&author=Garibo%2CD
- [22] "Yadav: Green synthesis of AgZnO nanoparticles: Structural... Google Scholar." Accessed: Sep. 27, 2023. [Online]. Available: https://scholar.google.com/scholar\_lookup?title=Green%20synthesis%20of%20AgZnO%20 nanoparticles%3A%20Structural%20analysis%2C%20hydrogen%20generation%2C%20for mylation%20and%20biodiesel%20applications&journal=J.%20Sci.%20Adv.%20Mater.%20 Devices&doi=10.1016%2Fj.jsamd.2019.03.001&volume=4&issue=3&pages=425-431&publication\_year=2019&author=Yadav%2CLR
- [23] S. G. Mtavangu, R. L. Machunda, B. van der Bruggen, and K. N. Njau, "In situ facile green synthesis of Ag–ZnO nanocomposites using Tetradenia riperia leaf extract and its antimicrobial efficacy on water disinfection," *Sci. Rep.*, vol. 12, no. 1, Art. no. 1, Sep. 2022, doi: 10.1038/s41598-022-19403-1.

- [24] F. Alharthi *et al.*, "Facile one-pot green synthesis of Ag–ZnO Nanocomposites using potato peeland their Ag concentration dependent photocatalytic properties," *Sci. Rep.*, vol. 10, Nov. 2020, doi: 10.1038/s41598-020-77426-y.
- [25] M. Barzegar, D. Ahmadvand, Z. Sabouri, and M. Darroudi, "Phytoextract-mediated synthesis of magnesium oxide nanoparticles using Caccinia macranthera extract and examination of their photocatalytic and anticancer effects," *Mater. Res. Bull.*, vol. 169, p. 112514, Jan. 2024, doi: 10.1016/j.materresbull.2023.112514.
- [26] M. A. Abomuti, E. Y. Danish, A. Firoz, N. Hasan, and M. A. Malik, "Green Synthesis of Zinc Oxide Nanoparticles Using Salvia officinalis Leaf Extract and Their Photocatalytic and Antifungal Activities," *Biology*, vol. 10, no. 11, p. 1075, Oct. 2021, doi: 10.3390/biology10111075.
- [27] A. H. Alrajhi, N. M. Ahmed, M. Al Shafouri, M. A. Almessiere, and A. ahmed Mohammed Al-Ghamdi, "Green synthesis of zinc oxide nanoparticles using salvia officials extract," *Mater. Sci. Semicond. Process.*, vol. 125, p. 105641, Apr. 2021, doi: 10.1016/j.mssp.2020.105641.
- [28] O. T. Fanoro *et al.*, "Biosynthesis of Smaller-Sized Platinum Nanoparticles Using the Leaf Extract of Combretum erythrophyllum and Its Antibacterial Activities," *Antibiotics*, vol. 10, no. 11, p. 1275, 2021.
- [29] J. Liu, J. Li, F. Wei, X. Zhao, Y. Su, and X. Han, "Ag–ZnO Submicrometer Rod Arrays for High-Efficiency Photocatalytic Degradation of Congo Red and Disinfection," *ACS Sustain. Chem. Eng.*, vol. 7, no. 13, pp. 11258–11266, Jul. 2019, doi: 10.1021/acssuschemeng.9b00610.
- [30] O. Bechambi, M. Chalbi, W. Najjar, and S. Sayadi, "Photocatalytic activity of ZnO doped with Ag on the degradation of endocrine disrupting under UV irradiation and the investigation of its antibacterial activity," *Appl. Surf. Sci.*, vol. 347, pp. 414–420, Aug. 2015, doi: 10.1016/j.apsusc.2015.03.049.
- [31] P. Pascariu *et al.*, "Photocatalytic and antimicrobial activity of electrospun ZnO:Ag nanostructures," *J. Alloys Compd.*, vol. 834, p. 155144, Sep. 2020, doi: 10.1016/j.jallcom.2020.155144.
- [32] S. Rajeshkumar, R. P. Parameswari, D. Sandhiya, K. A. Al-Ghanim, M. Nicoletti, and M. Govindarajan, "Green Synthesis, Characterization and Bioactivity of Mangifera indica Seed-Wrapped Zinc Oxide Nanoparticles," *Molecules*, vol. 28, no. 6, Art. no. 6, Jan. 2023, doi: 10.3390/molecules28062818.
- [33] S. Vimalraj, T. Ashokkumar, and S. Saravanan, "Biogenic gold nanoparticles synthesis mediated by Mangifera indica seed aqueous extracts exhibits antibacterial, anticancer and anti-angiogenic properties," *Biomed. Pharmacother.*, vol. 105, pp. 440–448, 2018.
- [34] "Suwarno: Biosynthesis of Dy2O3 nanoparticles using... Google Scholar." Accessed: Sep. 27, 2023. [Online]. Available: https://scholar.google.com/scholar\_lookup?title=Biosynthesis%20of%20Dy2O3%20nanopar ticles%20using%20Piper%20Retrofractum%20Vahl%20extract%3A%20Optical%2C%20str uctural%2C%20morphological%2C%20and%20photocatalytic%20properties&journal=J.%2 0Mol.%20Struct.&doi=10.1016%2Fj.molstruc.2022.133123&volume=1264&publication\_ye ar=2022&author=Suwarno%2CAC
- [35] "Surya: SmMnO3-decorated ZnO in a hexane-water interface... Google Scholar." Accessed: Sep. 27, 2023. [Online]. Available: https://scholar.google.com/scholar\_lookup?title=SmMnO3-decorated%20ZnO%20in%20a%20hexane-

- water% 20interface% 20for% 20enhancing% 20visible% 20light-driven% 20photocatalytic% 20degradation% 20of% 20malachite% 20green&journal=Chemosphere&doi=10.1016% 2Fj.chemosphere.2022.135125&volume=304&publication\_year=2022&author=Surya% 2CRM
- [36] "Yulizar: Fabrication of novel SnWO4/ZnO using Muntingia... Google Scholar." Accessed: Sep. 27, 2023. [Online]. Available: https://scholar.google.com/scholar\_lookup?title=Fabrication%20of%20novel%20SnWO4%2 FZnO%20using%20Muntingia%20calabura%20L.%20leaf%20extract%20with%20enhance d%20photocatalytic%20methylene%20blue%20degradation%20under%20visible%20light%20irradiation&journal=Ceram.%20Int.&doi=10.1016%2Fj.ceramint.2021.10.135&volume=4 8&issue=3&pages=3564-3577&publication\_year=2022&author=Yulizar%2CY&author=Apriandanu%2CDOB&author=Surya%2CRM
- [37] "Zare: Novel green biomimetic approach for synthesis... Google Scholar." Accessed: Sep. 27, 2023. [Online]. Available: https://scholar.google.com/scholar\_lookup?title=Novel%20green%20biomimetic%20approach%20for%20synthesis%20of%20ZnO-Ag%20nanocomposite%3B%20antimicrobial%20activity%20against%20foodborne%20pathogen%2C%20biocompatibility%20and%20solar%20photocatalysis&journal=Sci.%20Rep.&doi=10.1038%2Fs41598-019-44309-w&volume=9&issue=1&pages=1-15&publication\_year=2019&author=Zare%2CM
- [38] K. Ravichandran, R. Mohan, N. J. Begum, K. Swaminathan, and C. Ravidhas, "Property enhancement of transparent conducting zinc oxide thin films—Effect of simultaneous (Sn+F) doping," *J. Phys. Chem. Solids*, vol. 74, no. 12, pp. 1794–1801, Dec. 2013, doi: 10.1016/j.jpcs.2013.07.010.
- [39] M. Alkasir, N. Samadi, Z. Sabouri, Z. Mardani, M. Khatami, and M. Darroudi, "Evaluation cytotoxicity effects of biosynthesized zinc oxide nanoparticles using aqueous Linum Usitatissimum extract and investigation of their photocatalytic activityackn," *Inorg. Chem. Commun.*, vol. 119, p. 108066, Sep. 2020, doi: 10.1016/j.inoche.2020.108066.
- [40] M. A. Kareem, I. T. Bello, H. A. Shittu, P. Sivaprakash, O. Adedokun, and S. Arumugam, "Synthesis, characterization, and photocatalytic application of silver doped zinc oxide nanoparticles," *Clean. Mater.*, vol. 3, p. 100041, Mar. 2022, doi: 10.1016/j.clema.2022.100041.
- [41] E. R. Essien, V. N. Atasie, T. O. Oyebanji, and D. O. Nwude, "Biomimetic synthesis of magnesium oxide nanoparticles using Chromolaena odorata (L.) leaf extract," *Chem. Pap.*, vol. 74, no. 7, pp. 2101–2109, Jul. 2020, doi: 10.1007/s11696-020-01056-x.
- [42] S. Slathia, T. Gupta, and R. P. Chauhan, "Green synthesis of Ag–ZnO nanocomposite using Azadirachta indica leaf extract exhibiting excellent optical and electrical properties," *Phys. B Condens. Matter*, vol. 621, p. 413287, Nov. 2021, doi: 10.1016/j.physb.2021.413287.
- [43] S. Vijayakumar, B. Vaseeharan, B. Malaikozhundan, and M. Shobiya, "Laurus nobilis leaf extract mediated green synthesis of ZnO nanoparticles: characterization and biomedical applications," *Biomed. Pharmacother.*, vol. 84, pp. 1213–1222, 2016.
- [44] G. S, A. Gemta, C. AR, and Z. Belay, "Synthesis and Characterizations of Zinc Oxide Nanoparticles for Antibacterial Applications," *J. Nanomedicine Nanotechnol.*, vol. s8, Jan. 2017, doi: 10.4172/2157-7439.S8-004.

- [45] G. Nagaraju *et al.*, "Electrochemical heavy metal detection, photocatalytic, photoluminescence, biodiesel production and antibacterial activities of Ag–ZnO nanomaterial," *Mater. Res. Bull.*, vol. 94, pp. 54–63, Oct. 2017, doi: 10.1016/j.materresbull.2017.05.043.
- [46] Z. Yang and C. Xie, "Zn2+ release from zinc and zinc oxide particles in simulated uterine solution," *Colloids Surf. B Biointerfaces*, vol. 47, no. 2, pp. 140–145, Feb. 2006, doi: 10.1016/j.colsurfb.2005.12.007.
- [47] S. Soren, S. Kumar, S. Mishra, P. K. Jena, S. K. Verma, and P. Parhi, "Evaluation of antibacterial and antioxidant potential of the zinc oxide nanoparticles synthesized by aqueous and polyol method," *Microb. Pathog.*, vol. 119, pp. 145–151, Jun. 2018, doi: 10.1016/j.micpath.2018.03.048.
- [48] S. Nair *et al.*, "Role of size scale of ZnO nanoparticles and microparticles on toxicity toward bacteria and osteoblast cancer cells," *J. Mater. Sci. Mater. Med.*, vol. 20, no. 1, pp. 235–241, Dec. 2009, doi: 10.1007/s10856-008-3548-5.
- [49] Happy Agarwal, Soumya Menon, S. Venkat Kumar, and S. Rajeshkumar, "Mechanistic study on antibacterial action of zinc oxide nanoparticles synthesized using green route," *Chem. Biol. Interact.*, vol. 286, pp. 60–70, Apr. 2018, doi: 10.1016/j.cbi.2018.03.008.
- [50] C. Jayaseelan *et al.*, "Novel microbial route to synthesize ZnO nanoparticles using Aeromonas hydrophila and their activity against pathogenic bacteria and fungi," *Spectrochim. Acta. A. Mol. Biomol. Spectrosc.*, vol. 90, pp. 78–84, 2012.
- [51] S. M. Mousavi-Kouhi, A. Beyk-Khormizi, M. S. Amiri, M. Mashreghi, and M. E. T. Yazdi, "Silver-zinc oxide nanocomposite: From synthesis to antimicrobial and anticancer properties," *Ceram. Int.*, vol. 47, no. 15, pp. 21490–21497, 2021.
- [52] B. A. Abbasi *et al.*, "Bioactivities of Geranium wallichianum Leaf Extracts Conjugated with Zinc Oxide Nanoparticles," *Biomolecules*, vol. 10, no. 1, Art. no. 1, Jan. 2020, doi: 10.3390/biom10010038.
- [53] Ş. YEŞİLOT and S. DÖNMEZ, "Cytotoxic effect of green synthesized silver nanoparticles with Salvia officinalis on MCF-7 human breast cancer cells," *Turk. J. Health Sci. Life*, vol. 4, no. 3, pp. 133–139, 2021.
- [54] F. Sharifi, F. Sharififar, S. Soltanian, M. Doostmohammadi, and N. Mohamadi, "Synthesis of silver nanoparticles using Salvia officinalis extract: Structural characterization, cytotoxicity, antileishmanial and antimicrobial activity," *Nanomedicine Res. J.*, vol. 5, no. 4, pp. 339–346, 2020.